

G. H. Vineyard, Phys. Rev. **120**, 1229 (1960).

⁴M. W. Thompson, Phil. Mag. **4**, 139 (1959).

⁵M. W. Thompson and R. S. Nelson, Atomic Energy Research Establishment Report AERE-R 3320, 1960 (unpublished).

⁶D. O. Thompson, T. H. Blewitt, and D. K. Holmes, J. Appl. Phys. **28**, 275 (1957).

⁷R. S. Barnes, Phil. Mag. **5**, 635 (1960).

⁸J. Silcox, Proceedings of the European Regional Conference on Electron Microscopy, Delft, 1960 (to be published).

⁹A. Grenall, North American Aviation Report NAA-SR-5062 (unpublished).

¹⁰G. R. Piercy, Phil. Mag. **5**, 635 (1960).

SUPERCONDUCTIVITY OF Nb₃Sn IN A PULSED MAGNETIC FIELD*

J. O. Betterton, Jr., R. W. Boom, G. D. Kneip, and R. E. Worsham

Oak Ridge National Laboratory,[†] Oak Ridge, Tennessee

and

C. E. Roos

Vanderbilt University, Nashville, Tennessee

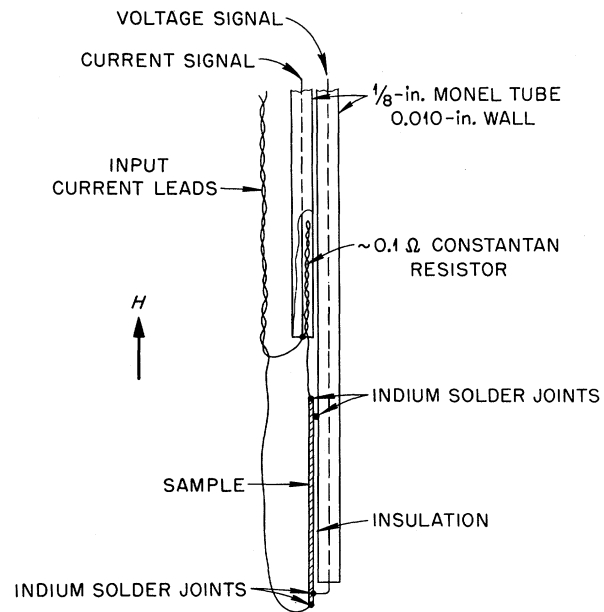
(Received April 24, 1961).

Kunzler, Buehler, Hsu, and Wernick¹ have shown that quenching of superconductivity in a niobium-clad wire with a Nb₃Sn core occurs at magnetic field strengths greater than 88 kilogauss and at core current densities in excess of 10⁵ amp/cm². Samples of this wire were prepared by methods suggested in reference 1. Critical current as a function of field was measured by a pulsed-field, pulsed-current method at 4.2°K in the Vanderbilt University 200-kilogauss magnet. The transition time from superconducting to normal state and the resistance were also determined.

A longitudinal specimen (0.38-mm diam and 2.5 cm long) and a constantan standard resistor were mounted at the end of two pieces of 3-mm diam, thin-wall Monel tubing as shown in Fig. 1. The Monel tubes served as the outer shields of coaxial lines which carried the sample voltage and current signals. A pickup coil to measure the field strength was placed adjacent to the test samples. The coils of the Vanderbilt magnet are arranged in a Helmholtz configuration to provide a field uniform to 2% over an experimental volume of 30 cm³. Current pulses of 30 to 150 microseconds were used at the peak of the magnetic field (half-period 1.2 milliseconds). The magnetic field was constant to within 2% during the longest current pulses. By mounting the sample as noninductively as practicable, a resistive sensitivity of 10 μohm was achieved, as checked with copper samples at a series of temperatures. A transverse specimen was mounted in a similar way.

Typical oscilloscope traces of the measured

current and voltage are shown in Fig. 2. In the upper set, the voltage across the sample illustrates a purely inductive response for a nonresistive superconductor. In the lower set, the voltage across the sample increases abruptly when the sample becomes resistive. The critical current is determined by measuring the current at the point where a resistive component is first detected. After the inductive voltage is subtracted, the normal-state resistance is approximately



Longitudinal Mount

FIG. 1. Specimen holder.

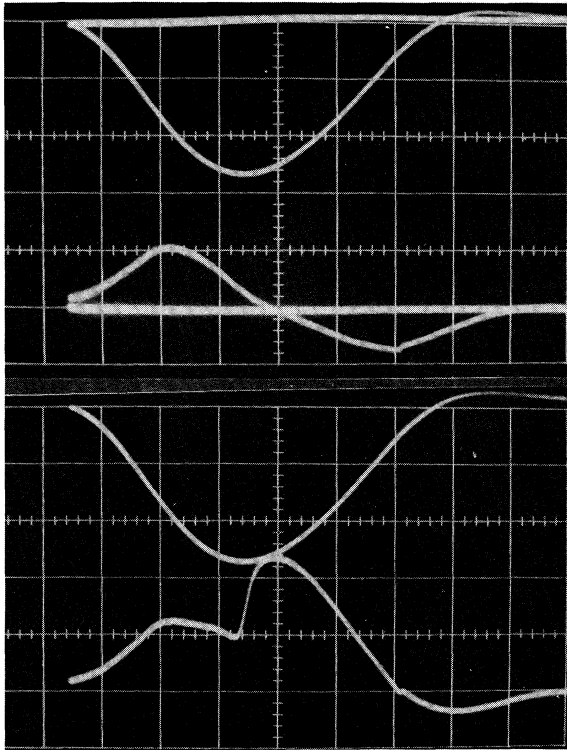


FIG. 2. Upper set: superconducting sample, $L di/dt$ response. Lower set: superconducting-to-normal transition, $L(di/dt) + iR$ response. Top traces: sample current, 89.5 amp/cm, positive direction downward. Bottom traces: sample voltage, 100 mv/cm, positive direction upward.

one milliohm. Both the transition time and the normal resistance depend on the previous history of the sample. Resistances as small as $10 \mu\text{ohm}$ and transition times as short as $2 \mu\text{sec}$ were observed. These effects are being investigated and will be reported in a later communication.

The critical current was plotted as a function of field for two samples; see Fig. 3. Sample No. 1 was measured both parallel and transverse to the field, while sample No. 2 was oriented parallel to the field only. The curves show that all samples carry currents of 210 to 260 amp in a zero external field. Sample No. 1 carries 100 amp at 100 kilogauss with the field parallel to the wire axis. A much smaller critical current occurs with the field oriented in a transverse direction. Both the current-carrying capacity and the maximum field at which current is carried are lower in sample No. 2. The difference between speci-

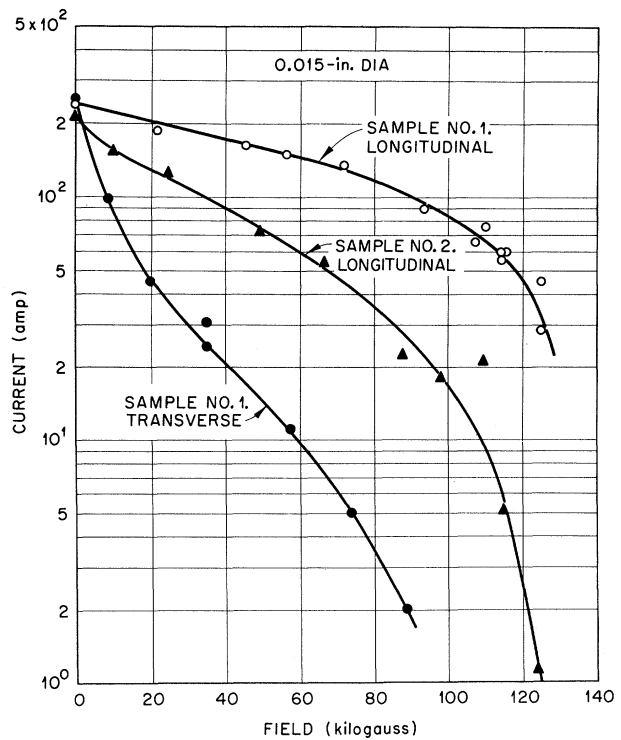


FIG. 3. Critical current vs applied magnetic field for Nb-Nb₃Sn wires at 4.2°K. (Wire diameter, 0.038 cm; core diameter, 0.015 cm.)

mens, shown in Fig. 3, is not entirely unexpected; the properties of hard superconductors are known to vary with slight differences of strain and defect structure.

Domain structure would appear to explain the differences obtained for parallel and transverse orientations. Only a small volume of the Nb₃Sn is superconducting at higher fields according to the magnetization curve of Bozorth, Williams, and Davis.² Studies of the intermediate state of various superconductors by Schawlow,³ DeSorbo,⁴ and Haenssler and Rinderer⁵ suggest that the internal structure tends to become arranged in domains with interfaces parallel to the field and normal to the current. A domain structure of this type in Nb-Nb₃Sn could account for the much smaller critical currents for transverse orientation. This can explain the differences found between the transverse and parallel orientations in soft superconductors. In a hard superconductor such as Nb₃Sn, however, the superconducting regions should be determined primarily by the macroscopic physical structure of the specimen.

Since this structure is oriented along the axis of the wire, it is somewhat surprising that such large differences between the parallel and transverse orientations were found.

The critical current at zero external field was also measured with direct currents in the samples. The direct-current values were 1/3 lower than those obtained with pulsed techniques. This is attributed to heating at the current joints or in the cladding which surrounds the Nb₃Sn core. This heating is substantially reduced with pulse techniques.

*Work supported in part by the National Science

Foundation and T. E. A. S. P.

†Operated for the U. S. Atomic Energy Commission by the Union Carbide Corporation.

¹J. E. Kunzler, E. Buehler, F. S. Hsu, and J. H. Wernick, *Phys. Rev. Letters* **6**, 89 (1961).

²R. M. Bozorth, A. J. Williams, and D. D. Davis, *Phys. Rev. Letters* **5**, 148 (1960).

³A. L. Schawlow, *Phys. Rev.* **101**, 573 (1956).

⁴W. DeSorbo, *Proceedings of the Seventh International Conference on Low-Temperature Physics* (University of Toronto Press, Toronto, Canada, 1960).

⁵F. Haenssler and L. Rinderer, *Proceedings of the Seventh International Conference on Low-Temperature Physics* (University of Toronto Press, Toronto, Canada, 1960).

FERMI SURFACE TOPOLOGY OF EVEN-VALENT METALS FROM THEIR MAGNETORESISTANCE ANISOTROPY

E. Fawcett

Physics Department, Royal Radar Establishment, Malvern, England
(Received March 27, 1961)

The anisotropy of the magnetoresistance of Au and Cu has recently been successfully interpreted by employing the concept of open orbits on a multiply-connected Fermi surface in a periodically extended zone scheme.¹ Open orbits occur for a limited range of field directions, and the transverse magnetoresistance $\rho_{\alpha\alpha}$ in a sufficiently high field H with the current making an angle α with the direction of the open orbits is then of the form,²

$$\rho_{\alpha\alpha} = A + BH^2 \cos^2 \alpha. \quad (1)$$

A plot of the resistance in a fixed high field whose direction varies is characterized by sharp maxima for field directions permitting some open orbits (with $\alpha \neq \pi/2$), which rise above the low resistance obtained for most field directions for which only closed orbits occur and the resistance saturates.

This behavior is in marked contrast with the anisotropy of the magnetoresistance observed for Mg,³ Zn,⁴ Cd,⁴ Pb,⁵ and Sn⁵ (the transition metals are not considered here and insufficient data are available for other even-valent metals). For these metals the resistance varies quadratically with field and is uniformly high for most field directions, falling to sharp minima for certain field directions where it varies less rapidly.

The proposed explanation of this behavior in the even-valent metals is as follows. Consider the range of field directions for which closed cyclo-

tron orbits occur over the whole Fermi surface, and fields so large that for all such orbits $\omega_c \bar{\tau} \gg 1$, ω_c being the cyclotron frequency and $\bar{\tau}$ the relaxation time averaged over the orbit. If the component σ_{xy} of the conductivity tensor with field H along the z axis is expanded in ascending powers of $1/H$, the leading term is of the form,²

$$\sigma_{xy} = -\frac{e}{cH} \frac{2}{\hbar^3} \sum_i \int S_i(p_z) dp_z. \quad (2)$$

Here the area $S_i(p_z)$ enclosed by the intersections with the sheet i of the Fermi surface by the plane $p_z = \text{constant}$ will, in general, be the sum of positive terms for closed orbits containing occupied electron states of lower energy within and immediately adjacent to each orbit, and of negative terms for orbits containing hole states. For the case where all sheets of the Fermi surface are simply connected, the range of integration need be only over a single Brillouin zone (with suitable remapping), and Eq. (2) results in the well-known expression,²⁻⁶

$$\sigma_{xy} = -\frac{e}{cH} (n_e - n_h) N_a. \quad (3)$$

Here N_a is the number of atoms per unit volume, and n_e and n_h are the numbers of electron and hole states per atom, which are well defined since each sheet consists of closed surfaces containing either electrons or holes.

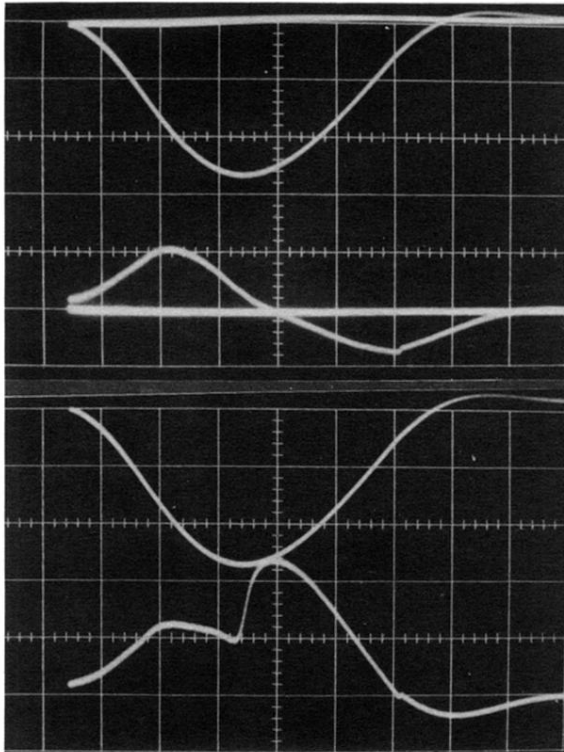


FIG. 2. Upper set: superconducting sample, $L di/dt$ response. Lower set: superconducting-to-normal transition, $L(di/dt) + iR$ response. Top traces: sample current, 89.5 amp/cm, positive direction downward. Bottom traces: sample voltage, 100 mv/cm, positive direction upward.